

A QCD-like theory with the \mathbb{Z}_{N_c} symmetry

Hiroaki Kouno,^{1,*} Yuji Sakai,^{2,†} Takahiro Makiyama,¹ Kouhei Tokunaga,¹ Takahiro Sasaki,^{2,‡} and Masanobu Yahiro^{2,§}

¹*Department of Physics, Saga University, Saga 840-8502, Japan*

²*Department of Physics, Graduate School of Sciences, Kyushu University, Fukuoka 812-8581, Japan*

(Dated: October 21, 2018)

We propose a QCD-like theory with the \mathbb{Z}_{N_c} symmetry. The flavor-dependent twisted boundary condition (TBC) is imposed on N_c degenerate flavor quarks in the $SU(N_c)$ gauge theory. The QCD-like theory is useful to understand the mechanism of color confinement. Dynamics of the QCD-like theory is studied by imposing the TBC on the Polyakov-loop extended Nambu-Jona-Lasinio (PNJL) model. The TBC model is applied to two- and three-color cases. The \mathbb{Z}_{N_c} symmetry is preserved below some temperature T_c , but spontaneously broken above T_c . The color confinement below T_c preserves the flavor symmetry. Above T_c , the flavor symmetry is broken, but the breaking is suppressed by the entanglement between the Polyakov loop and the chiral condensate. Particularly at low temperature, dynamics of the TBC model is similar to that of the PNJL model with the standard fermion boundary condition, indicating that the \mathbb{Z}_{N_c} symmetry is a good approximate concept in the latter model even if the current quark mass is small. The present prediction can be tested in future by lattice QCD, since the QCD-like theory has no sign problem.

PACS numbers: 11.30.Rd, 12.40.-y

I. INTRODUCTION.

Understanding of the confinement mechanism is one of the most important subjects in hadron physics. According to Lattice QCD (LQCD), the system is in the confinement and chiral symmetry breaking phase at low temperature (T), but in the deconfinement and chiral symmetry restoration phase at high T . The confinement mechanism is, nevertheless, still unclear for several reasons. The main reason is that the exact symmetry is not found for the deconfinement transition and hence the order parameter is unknown. In the limit of zero current quark mass, the chiral condensate is an exact order parameter for the chiral restoration. In the limit of infinite current quark mass, on the contrary, the Polyakov loop becomes an exact order parameter for the deconfinement transition, since the \mathbb{Z}_{N_c} symmetry is exact there. For the real world in which u and d quarks have small current quark masses, the chiral condensate is considered to be a good order parameter, but it is not clear whether the Polyakov loop is a good order parameter. In this paper, we approach this problem by proposing a QCD-like theory with the \mathbb{Z}_{N_c} symmetry.

We start with the $SU(N_c)$ gauge theory with N_f degenerate flavor quarks. The partition function Z in Euclidean space-time is described by

$$Z = \int Dq D\bar{q} DA \exp[-S_0] \quad (1)$$

with the action

$$S_0 = \int d^4x \left[\sum_f \bar{q}_f (\gamma_\nu D_\nu + m_f) q_f + \frac{1}{4g^2} F_{\mu\nu}^a{}^2 \right], \quad (2)$$

where q_f is the quark field with flavor f and current quark mass m_f , $D_\nu = \partial_\nu + iA_\nu$ is the covariant derivative with the gauge field A_ν , g is the gauge coupling and $F_{\mu\nu} = \partial_\mu A_\nu - \partial_\nu A_\mu - i[A_\mu, A_\nu] = F_{\mu\nu}^a T^a$ with the $SU(N_c)$ generator T^a . The temporal boundary condition for quark is

$$q_f(x, \beta = 1/T) = -q_f(x, 0). \quad (3)$$

The \mathbb{Z}_{N_c} transformation changes the fermion boundary condition as [1, 2]

$$q_f(x, \beta) = -\exp(-i2\pi k/N_c) q_f(x, 0) \quad (4)$$

for integer k , while the action S_0 keeps the original form (2) since the \mathbb{Z}_{N_c} symmetry is the center symmetry of the gauge symmetry [1]. The \mathbb{Z}_{N_c} symmetry thus breaks down through the fermion boundary condition in QCD.

Now we consider the $SU(N)$ gauge theory with N degenerate flavor quarks, i.e. $N \equiv N_f = N_c$, and assume the following twisted boundary conditions (TBC):

$$\begin{aligned} q_f(x, \beta) &= -\exp(i\theta_f) q_f(x, 0) \\ &\equiv -\exp[i(\theta_1 + 2\pi(f-1)/N)] q_f(x, 0) \end{aligned} \quad (5)$$

for flavors f labeled by integers from 1 to N ; see Fig.1 for the twisted angles θ_f . Here θ_1 is an arbitrary real number in a range of $0 \leq \theta_1 < 2\pi$. The action S_0 with the TBC is not QCD but a QCD-like theory. The QCD-like theory has the \mathbb{Z}_{N_c} symmetry, i.e. invariant under the \mathbb{Z}_{N_c} transformation. In fact, the \mathbb{Z}_{N_c} transformation changes f into $f - k$, but $f - k$ can be relabeled by f since S_0 is invariant under the relabeling. The QCD-like theory with the \mathbb{Z}_{N_c} symmetry is useful to understand the mechanism of color confinement.

When the fermion field q_f is transformed by

$$q_f \rightarrow \exp(-i\theta_f T \tau) q_f \quad (6)$$

for Euclidean time τ , the action S_0 is changed into

$$S(\theta_f) = \int d^4x \left[\sum_f \bar{q}_f (\gamma_\nu D_\nu - \mu_f \gamma_4 + m_f) q_f + \frac{1}{4g^2} F_{\mu\nu}^a{}^2 \right] \quad (7)$$

*kounoh@cc.saga-u.ac.jp

†sakai@phys.kyushu-u.ac.jp

‡sasaki@phys.kyushu-u.ac.jp

§yahiro@phys.kyushu-u.ac.jp

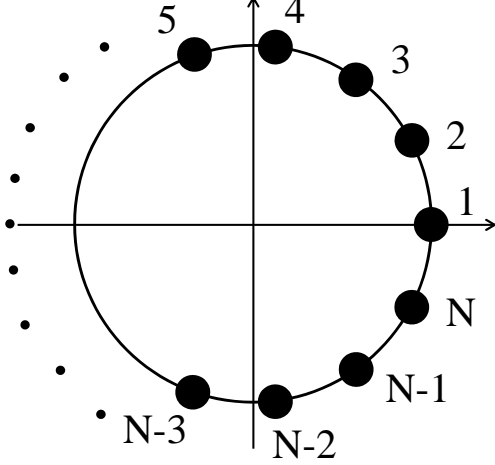


Fig. 1: Twisted factors $e^{i\theta_f}$ ($f = 1, 2, \dots, N$) on a unit circle in the complex plane for the case of $\theta_1 = 0$.

with the imaginary quark number chemical potential $\mu_f = iT\theta_f$, while the TBC is transformed back to the standard one (3). The action S_0 with the TBC is thus equivalent to the action $S(\theta_f)$ with the standard one (3). In the limit of $T = 0$, the action $S(\theta_f)$ tends to S_0 with (3) fixed. The QCD-like theory is thus identical with QCD at $T = 0$ where the Polyakov loop Φ is zero. This indicates that in the QCD-like theory the \mathbb{Z}_{N_c} symmetry is preserved up to some temperature T_c and spontaneously broken above T_c . In the QCD-like theory, the flavor symmetry is explicitly broken by the flavor-dependent TBC. As shown later, the flavor-symmetry breaking is recovered below T_c . The breaking then becomes significant only above T_c .

In general, the QCD partition function $Z(T, \theta)$ with finite imaginary chemical potential θ has the Roberge-Weiss (RW) periodicity [1]: $Z(T, \theta) = Z(T, \theta + 2\pi k/N_c)$ for any integer k . The RW periodicity was confirmed by lattice QCD (LQCD) [3–12] and the Holographic QCD [13]. The RW periodicity means that $Z(T, \theta)$ is invariant under the extended \mathbb{Z}_{N_c} transformation, i.e. the combination of the \mathbb{Z}_{N_c} transformation and the parameter transformation $\theta \rightarrow \theta + 2\pi k/N_c$. Actually, $Z(T, \theta)$ is transformed into $Z(T, \theta - 2\pi k/N_c)$ by the \mathbb{Z}_{N_c} transformation and $Z(T, \theta - 2\pi k/N_c)$ is transformed back to $Z(T, \theta)$ by the parameter transformation. The QCD partition function thus has the extended \mathbb{Z}_{N_c} symmetry, and dynamics of QCD at imaginary chemical potential is governed by the symmetry.

The extended \mathbb{Z}_{N_c} symmetry is not an internal symmetry, since the transformation includes the shift of external parameter θ . In the QCD-like theory, the shift of θ is not necessary because of the TBC. Thus the QCD-like theory possesses the \mathbb{Z}_{N_c} symmetry as an internal symmetry, whereas QCD has the extended \mathbb{Z}_{N_c} symmetry as an external symmetry. The Polyakov-loop extended Nambu-Jona-Lasinio (PNJL) model [2, 14–51] is a good model to understand QCD at finite imaginary chemical potential θ and hence the QCD-

like theory, since the PNJL model possesses the extended \mathbb{Z}_{N_c} symmetry in the standard fermion boundary condition (3) [2].

In this paper, we propose a QCD-like theory with the \mathbb{Z}_{N_c} symmetry. The theory is constructed by imposing the TBC on the $SU(N_c)$ gauge theory with N_c degenerate flavor quarks. Dynamics of the QCD-like theory is studied concretely by imposing the TBC on the PNJL model. Two cases of $N_c = N_f = 2$ and 3 are mainly considered. In this paper, the PNJL model with the TBC is shortly called the TBC model, and the PNJL model with the standard boundary condition is named the standard-PNJL model. We first show that the \mathbb{Z}_{N_c} symmetry is preserved below some temperature T_c , but spontaneously broken above T_c . The interplay between the \mathbb{Z}_{N_c} symmetry breaking and the flavor symmetry breaking is investigated. Comparing the deconfinement transition in the TBC model with that in the standard-PNJL model, we show that the \mathbb{Z}_{N_c} symmetry is a good approximate concept in the latter model, even if the current quark mass is small. The present prediction can be checked by LQCD in future, since LQCD with the TBC is free from the sign problem.

This paper is organized as follows. The case of $N_c = N_f = 2$ is investigated in Sec. II and that of $N_c = N_f = 3$ is in Sec. III. Two interesting extensions of the TBC model are shown in Sec. IIIC. Section IV is devoted to summary.

II. CASE OF $N_c = 2$

A. Formalism

The two-color and two-flavor PNJL Lagrangian [34] in Euclidean spacetime is

$$\begin{aligned} \mathcal{L} &= \sum_f \bar{q}_f (\gamma_\nu D_\nu - \mu_f \gamma_4 + m_f) q_f \\ &- (1 - \alpha) G_s \sum_f \sum_{a=0}^3 [(\bar{q}_f \tau_a q_f)^2 + (\bar{q}_f i \gamma_5 \tau_a q_f)^2] \\ &+ 4\alpha G_s \left[\det_{ij} (\bar{q}_i (1 + \gamma_5) q_j) + \det_{ij} (\bar{q}_i (1 - \gamma_5) q_j) \right] \\ &+ \mathcal{U}(\Phi[A], \Phi[A]^*, T) \end{aligned} \quad (8)$$

with $D_\nu = \partial_\nu + iA_\nu = \partial_\nu + i\delta_{\nu,4} A_{4,a} \frac{\tilde{\tau}_a}{2}$ for the gauge field A_a^ν , where the τ_a ($\tilde{\tau}_a$) for $a = 1, 2, 3$ are the Pauli matrices in flavor (color) space and τ_0 is the unit matrix in flavor space. In the NJL sector, $(1 - \alpha)G_s$ denotes coupling constants of scalar- and pseudoscalar-type four-quark interactions, whereas αG_s is that of the Kobayashi-Maskawa-'t Hooft determinant interaction [52, 53]. Here α can vary from 0 to 1/2 for positive G_s . The $U_A(1)$ anomaly vanishes when $\alpha = 0$. The Polyakov potential \mathcal{U} , defined in (11), is a function of the Polyakov loop Φ and its Hermitian conjugate Φ^* . The parameter m_f (μ_f) stands for the current quark mass (the chemical potential) for each flavor. Here we set $m_0 \equiv m_u = m_d$.

In the PNJL model, the gauge field A_μ is treated as a homogeneous and static background field [16, 34]. In the case

of $N_c = 2$, the Polyakov-loop $\bar{\Phi}$ and its conjugate Φ^* are determined in Euclidean spacetime by

$$\bar{\Phi} = \frac{1}{2}\text{tr}_c(L), \quad \Phi^* = \frac{1}{2}\text{tr}_c(\bar{L}), \quad (9)$$

where $L = \exp(iA_4/T)$ with $A_4 = iA_0$. In the Polyakov-gauge, A_4 is diagonal in color space, i.e., $A_4/T = \text{diag}(\phi_1, \phi_2)$ for the ϕ_i satisfying $\phi_1 + \phi_2 = 0$. This leads to

$$\begin{aligned} \bar{\Phi} &= \frac{1}{2}(e^{i\phi_1} + e^{i\phi_2}) \\ &= \frac{1}{2}(e^{i\phi_1} + e^{-i\phi_1}) = \cos(\phi_1), \\ \Phi^* &= \frac{1}{2}(e^{-i\phi_1} + e^{-i\phi_2}) \\ &= \frac{1}{2}(e^{-i\phi_1} + e^{i\phi_1}) = \cos(\phi_1) = \bar{\Phi}, \end{aligned} \quad (10)$$

indicating that $\bar{\Phi}$ is real. For the Polyakov-loop potential \mathcal{U} , we use

$$\mathcal{U} = -bT[24e^{-a/T}\bar{\Phi}^2 + \log(1 - \bar{\Phi}^2)] \quad (11)$$

proposed in Ref. [34], where $a = 858.1$ MeV and $b^{1/3} = 210.5$ MeV. The Polyakov potential yields the second-order deconfinement phase transition at $T_c = 270$ MeV in the pure gauge theory.

Now we consider the imaginary chemical potential $\mu_f = i\theta_f T$, where the twisted angles θ_f are real. Making the mean-field approximation (MFA) and the path integral over the quark fields in the PNJL partition function Z_{PNJL} , one can obtain the thermodynamic potential (per unit volume) as

$$\begin{aligned} \Omega &= -T \ln(Z_{\text{PNJL}})/V \\ &= -2 \sum_{f=u,d} \sum_{c=1,2} \int \frac{d^3p}{(2\pi)^3} \left[E_f \right. \\ &\quad \left. + \frac{1}{\beta} \ln [1 + e^{i\phi_c} e^{i\theta_f} e^{-\beta E_f}] \right. \\ &\quad \left. + \frac{1}{\beta} \ln [1 + e^{-i\phi_c} e^{-i\theta_f} e^{-\beta E_f}] \right] \\ &\quad + U(\sigma, a_0) + \mathcal{U}(\bar{\Phi}, T), \end{aligned} \quad (12)$$

where $E_f^\pm(\mathbf{p}) = E_f(\mathbf{p}) \pm \mu_f$ for $E_f(\mathbf{p}) = \sqrt{\mathbf{p}^2 + M_f^2}$,

$$M_u = m_0 - 2G_s(\sigma + \zeta a_0), \quad (13)$$

$$M_d = m_0 - 2G_s(\sigma - \zeta a_0), \quad (14)$$

$$U = G_s[\sigma^2 + \zeta a_0^2], \quad (15)$$

$\zeta = 1 - 2\alpha$, $\sigma = \langle \bar{u}u + \bar{d}d \rangle$ and $a_0 = \langle \bar{u}u - \bar{d}d \rangle$. Here only the flavor-diagonal scalar condensates are taken. On the right-hand side of (12) only the first term is regularized by the three-dimensional momentum cutoff Λ [16, 17], since it diverges.

The variables, $X = (\bar{\Phi}, \Phi^*, \sigma, a_0)$, are determined by the stationary conditions

$$\partial\Omega/\partial X = 0. \quad (16)$$

Solutions $X(T, \theta_f)$ of the conditions do not give a global minimum of Ω necessarily, when the solutions are inserted back to (12). There is a possibility that they yield a local minimum or even a maximum. We have then checked that the solutions yield a global minimum

Following Ref. [34], we take the parameter set of $m_0 = 5.4$ MeV, $\Lambda = 657$ MeV and $G_s = 7.23$ GeV² that yield $-\langle \bar{u}u \rangle^{1/3} = 218$ MeV, the pion decay constant $f_\pi = 75.4$ MeV and the pion mass $m_\pi = 140$ MeV at vacuum.

Taking the summation over color indices in (12) leads to

$$\begin{aligned} \Omega &= -2 \sum_{f=u,d} \int \frac{d^3p}{(2\pi)^3} \left[2E_f \right. \\ &\quad \left. + \frac{1}{\beta} \ln [1 + C_{2,1}(\mathbf{p})e^{i\theta_f} + C_{2,2}(\mathbf{p})e^{2i\theta_f}] \right. \\ &\quad \left. + \frac{1}{\beta} \ln [1 + C_{2,1}(\mathbf{p})e^{-i\theta_f} + C_{2,2}(\mathbf{p})e^{-2i\theta_f}] \right] \\ &\quad + U(\sigma, a_0) + \mathcal{U}(\bar{\Phi}, T), \end{aligned} \quad (17)$$

where

$$\begin{aligned} C_{2,1}(\mathbf{p}) &= 2\bar{\Phi}e^{-\beta E_f}, \\ C_{2,2}(\mathbf{p}) &= e^{-2\beta E_f}. \end{aligned} \quad (18)$$

It is found from (18) that $C_{2,1} = 0$ and $C_{2,2} \neq 0$ when $\bar{\Phi} = 0$. The configuration means that two colored quarks are statistically in the same state. The configuration is thus realized as a result of the color confinement ($\bar{\Phi} = 0$). In other words, the color confinement can be defined by the configuration.

Making the \mathbb{Z}_2 transformation

$$\bar{\Phi} \rightarrow e^{-ik\pi} \bar{\Phi} \quad (19)$$

in (17), one can find that Ω has the RW periodicity,

$$\Omega(\theta_f) = \Omega(\theta_f + k\pi). \quad (20)$$

Namely, Ω has the extended \mathbb{Z}_2 symmetry. The TBC corresponds to setting $\theta_u = \theta_1$ and $\theta_d = \theta_1 + \pi$ in Ω . The \mathbb{Z}_2 symmetry with odd k changes (θ_u, θ_d) to (θ_d, θ_u) , but (θ_d, θ_u) returns to (θ_u, θ_d) by the relabeling of flavors. The TBC model thus has the \mathbb{Z}_2 symmetry as an internal symmetry in addition to the extended \mathbb{Z}_2 symmetry as an external symmetry.

In the color-confinement phase defined by $\bar{\Phi} = 0$, the thermodynamic potential Ω has only the configuration of $C_{2,1} = 0$ and $C_{2,2} \neq 0$, as mentioned above. Components including $C_{2,2}$ in (17) have flavor dependence only through factors $e^{\pm 2i\theta_f}$, but the factors has no flavor dependence because of $(\theta_u, \theta_d) = (\theta_1, \theta_1 + \pi)$. Noting that the M_f are determined by the stationary condition (16) from the flavor-independent Ω , one can see that the flavor symmetry is recovered by the color confinement.

B. Numerical results

Let us start with the standard-PNJL model, i.e., the PNJL model with no chemical potential. In this case, the Polykov

loop Φ is an approximate order parameter of the color confinement, while the chiral condensate σ is an approximate order parameter of the chiral transition. The flavor symmetry breaking is described by the isovector condensate a_0 . We mainly consider the $U_A(1)$ symmetric case by taking $\alpha = 0$.

Figure 2 shows T dependence of Φ and σ calculated with the standard-PNJL model, where σ is normalized by $\sigma_0 \equiv \sigma(T = 0, \mu_f = 0)$. Both σ and Φ are finite for any T , since there is no exact chiral and \mathbb{Z}_2 symmetry. As T increases, σ decreases gradually, while Φ increases smoothly. The chiral and deconfinement transitions are thus crossover. Here a_0 is zero at any T , since the flavor symmetry is not broken.

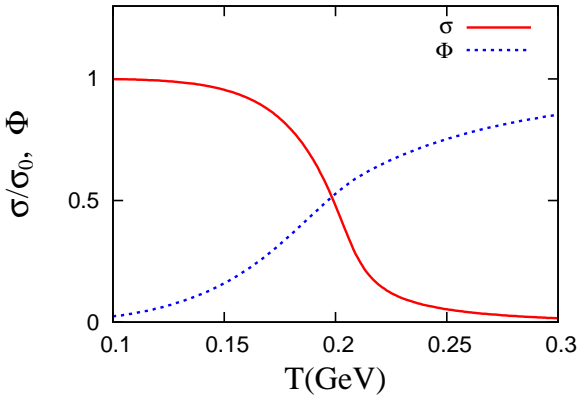


Fig. 2: T dependence of σ and Φ in the case of $\alpha = 0$ and $(\theta_u, \theta_d) = (0, 0)$. Here σ is normalized by $\sigma_0 \equiv \sigma(T = 0, \mu_f = 0)$.

Now we consider the TBC model with the \mathbb{Z}_2 symmetry. The Polyakov loop Φ is an exact order parameter of the color confinement. When $\Phi \neq 0$, there are two \mathbb{Z}_2 vacua. The vacuum with positive Φ is taken in this paper.

First we analyze the case

$$(\theta_u, \theta_d) = (-\pi/2, \pi/2) \quad (21)$$

corresponding to $\theta_1 = -\pi/2$ in the TBC of (5); see the right panel of Fig. 3 for the twisted angles. In this case, the flavor symmetry is not broken by the TBC, because

$$\Omega(\theta_u, \theta_d) = \Omega(-\theta_u, -\theta_d) = \Omega(\theta_d, \theta_u), \quad (22)$$

where the first and second equalities are obtained by the charge-conjugation and (21), respectively.

Figure 4 shows σ and Φ as a function of T ; note that a_0 is zero for any T because of the flavor symmetry. The Polyakov loop Φ is zero up to $T \equiv T_c \approx 260$ MeV, but finite above T_c . The \mathbb{Z}_2 symmetry is thus preserved exactly below T_c , but spontaneously broken above T_c . The deconfinement phase transition is second-order, since Φ has no jump at $T = T_c$. Meanwhile, the chiral transition is crossover. There is no qualitative difference between the standard-PNJL model and the TBC model with $\theta_1 = -\pi/2$ for the deconfinement and chiral transitions, although the order of the deconfinement transition becomes stronger by the exact \mathbb{Z}_2 symmetry.

In Fig. 5, the color state factors $C_{2,1}(\mathbf{p} = 0)$ and $C_{2,2}(\mathbf{p} = 0)$ are drawn as a function of T . The one-quark state $C_{2,1}(\mathbf{p} =$

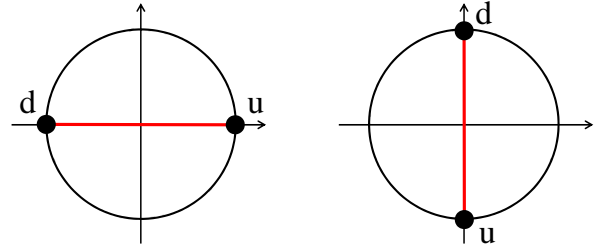


Fig. 3: Twisted factors $e^{i\theta_f}$ on a unit circle in the complex plane for the case of $\theta_1 = 0$ (left) and $\theta_1 = -\pi/2$ (right).

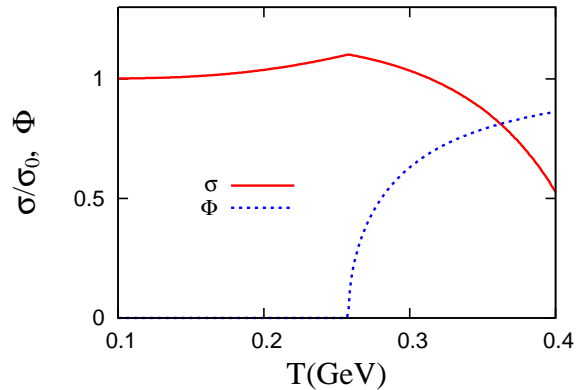


Fig. 4: T dependence of σ and Φ in the case of $\alpha = 0$ and $(\theta_u, \theta_d) = (-\pi/2, \pi/2)$. σ is normalized by σ_0 .

0) vanishes below T_c because of $\Phi = 0$. Above T_c , on the contrary, the system is dominated by the one-color state, although the two-quark state $C_{2,2}$ remains there.

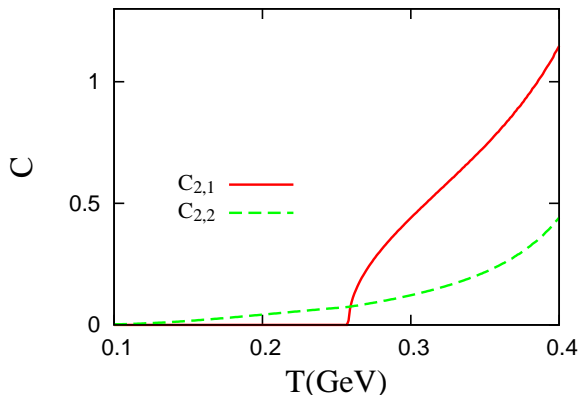


Fig. 5: T dependence of the color state factors $C_{2,1}(\mathbf{p} = 0)$ (solid line) and $C_{2,2}(\mathbf{p} = 0)$ (dashed line) in the case of $\alpha = 0$ and $(\theta_u, \theta_d) = (-\pi/2, \pi/2)$.

The delay of the chiral restoration at higher T can be under-

stood as follows. Taking the flavor summation in (12) leads to

$$\begin{aligned} \Omega = & -2 \sum_{c=1,2} \int \frac{d^3p}{(2\pi)^3} \left[N_c E_f \right. \\ & + \frac{1}{\beta} \ln [1 + F_{2,1}(\mathbf{p})e^{-\phi_c} + F_{2,2}(\mathbf{p})e^{-2i\phi_c}] \\ & + \frac{1}{\beta} \ln [1 + F_{2,1}^*(\mathbf{p})e^{i\phi_c} + F_{2,2}^*(\mathbf{p})e^{2i\phi_c}] \\ & \left. + U(\sigma, a_0) + \mathcal{U}(\Phi, T), \right. \end{aligned} \quad (23)$$

where

$$\begin{aligned} F_{2,1}(\mathbf{p}) &= e^{i\theta_u} e^{-\beta E_u} + e^{i\theta_d} e^{-\beta E_d}, \\ F_{2,2}(\mathbf{p}) &= e^{i(\theta_u + \theta_d)} e^{-\beta(E_u + E_d)}. \end{aligned} \quad (24)$$

Since $\theta_u = \theta_1$ and $\theta_d = \theta_1 + \pi$, Eq. (24) is reduced to

$$\begin{aligned} F_{2,1}(\mathbf{p}) &= e^{i\theta_1} (z_{2,1} e^{-\beta E_u} + z_{2,2} e^{-\beta E_d}), \\ F_{2,2}(\mathbf{p}) &= -e^{2i\theta_1} e^{-\beta(E_u + E_d)}, \end{aligned} \quad (25)$$

where $z_{2,1} = 1$ and $z_{2,2} = -1$ are elements of the \mathbb{Z}_2 group. In the case of $(\theta_u, \theta_d) = (-\pi/2, \pi/2)$, the flavor symmetry is not broken, so that $E \equiv E_u = E_d$. In this situation, $F_{2,1}$ and $F_{2,2}$ are further reduced to

$$\begin{aligned} F_{2,1}(\mathbf{p}) &= -i(z_{2,1} + z_{2,2}) e^{-\beta E} = 0 \\ F_{2,2}(\mathbf{p}) &= e^{-2\beta E}. \end{aligned} \quad (26)$$

The thermodynamic system thus has no $F_{2,1}$ but finite $F_{2,2}$. This means that u - and d -quarks are statistically in the same state. The chiral condensate σ has weak T dependence, since the two-quark state factor $F_{2,2}$ is strongly suppressed by the factor $\exp(-2\beta E)$. Eventually, the chiral restoration becomes much slower in the TBC model. This slow restoration is true also for the case of $N_c = 3$ and $N_f = 2$ [39], although the \mathbb{Z}_3 symmetry is not exact in the case.

Next we analyze the case

$$(\theta_u, \theta_d) = (0, \pi) \quad (27)$$

corresponding to $\theta_1 = 0$ in the TBC of (5); see the left panel of Fig. 3 for the twisted angles. Figure 6 presents T dependence of a_0 and Φ . In this case, the flavor symmetry is explicitly broken by the TBC. The second-order deconfinement phase transition occurs at $T = T_c \approx 235$ MeV. Below T_c , a_0 and Φ are zero, indicating that the flavor symmetry is restored by the color confinement. Above T_c , both a_0 and Φ become finite, indicating that the flavor and \mathbb{Z}_2 symmetries break simultaneously. At high T where the flavor symmetry breaking is strong, σ is getting large with respect to increasing T . This behavior is quite different from the corresponding behavior of σ in the standard-PNJL model.

Figure 7 shows T dependence of the constituent quark masses M_u and M_d . The quark masses are degenerate below T_c , but above T_c d -quark becomes heavier while u -quark does lighter. The mass splitting is a consequence of the flavor symmetry breaking.

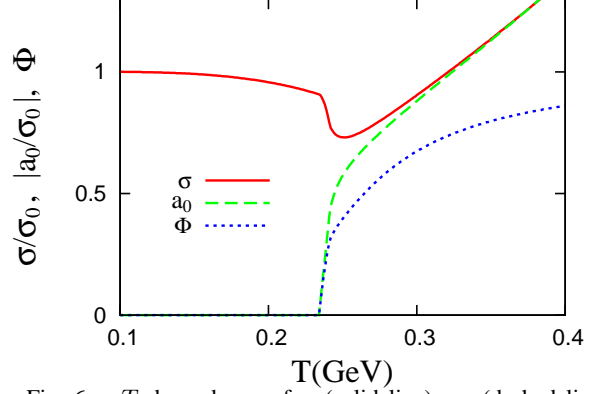


Fig. 6: T dependence of σ (solid line), a_0 (dashed line) and Φ (dotted line) in the case of $\alpha = 0$ and $(\theta_u, \theta_d) = (0, \pi)$. σ and a_0 are normalized by σ_0 . Note that $\sigma < 0$ and $a_0 \geq 0$.

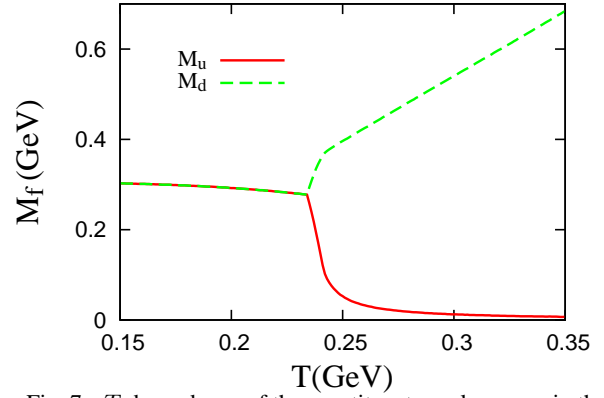


Fig. 7: T dependence of the constituent quark masses in the case of $\alpha = 0$ and $(\theta_u, \theta_d) = (0, \pi)$. The solid (dashed) line represents u (d) quark mass.

In Fig. 8, the color state factors $C_{2,1}(\mathbf{p} = 0)$ and $C_{2,2}(\mathbf{p} = 0)$ are plotted for u -quark as a function of T . Below T_c , only the two-quark state $C_{2,2}$ remains. Above T_c , the system is dominated by the one-quark state $C_{2,1}$.

Figure 9 shows T dependence of a_0 and Φ in the case of $\alpha = 0.2$. The T dependence is similar to that in the case of $\alpha = 0$, although $T_c \approx 265$ MeV in the former and 235 MeV in the latter. Comparing Fig. 9 with Fig. 6, one can see explicitly that T_c becomes larger as α increases. The $U_A(1)$ anomaly thus delays the spontaneous breaking of the \mathbb{Z}_2 symmetry and hence that of the flavor-symmetry breaking.

III. CASE OF $N_c = 3$

A. Formalism

The present formulation for $N_c = N_f = 3$ is parallel to that for $N_c = N_f = 2$ shown in Sec. II A. The PNJL Lagrangian

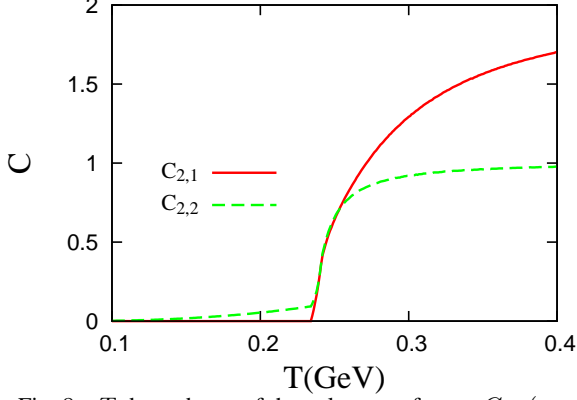


Fig. 8: T dependence of the color state factors $C_{2,1}(\mathbf{p} = 0)$ (solid line) and $C_{2,2}(\mathbf{p} = 0)$ (dashed line) for u quark in the case of $\alpha = 0$ and $(\theta_u, \theta_d) = (0, \pi)$.

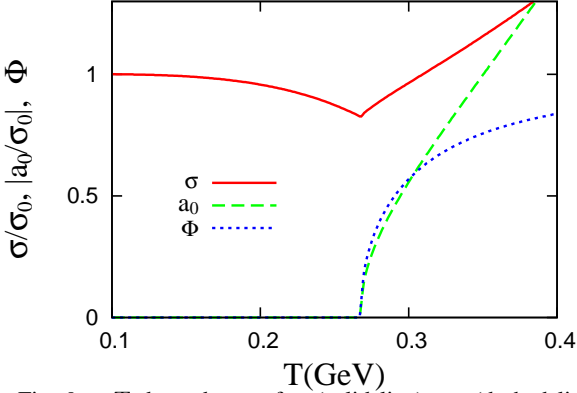


Fig. 9: T dependence of σ (solid line), a_0 (dashed line) and Φ (dotted line) in the case of $\alpha = 0.2$ and $(\theta_u, \theta_d) = (0, \pi)$. σ and a_0 are normalized by σ_0 . Note that $\sigma < 0$ and $a_0 \geq 0$.

with $N_c = N_f = 3$ is

$$\begin{aligned} \mathcal{L} = & \sum_f \bar{q}_f (\gamma_\nu D_\nu - \mu_f \gamma_4 + m_f) q_f \\ & - G_S \sum_f \sum_{a=0}^8 [(\bar{q}_f \lambda_a q_f)^2 + (\bar{q}_f i \gamma_5 \lambda_a q_f)^2] \\ & + G_D \left[\det_{ij} \bar{q}_i (1 + \gamma_5) q_j + \det_{ij} \bar{q}_i (1 - \gamma_5) q_j \right] \\ & + \mathcal{U}(\Phi[A], \bar{\Phi}[A], T), \end{aligned} \quad (28)$$

where $D_\nu = \partial_\nu + iA_\nu = \partial_\nu + i\delta_{\nu,4} A_{4,a} \tilde{\lambda}_a / 2$ with the Gell-Mann matrices $\tilde{\lambda}_a$ in color space. In the interaction part, λ_a ($a \neq 0$) and λ_0 are the Gell-Mann matrices and the unit matrix in flavor space, respectively, and G_S and G_D are coupling constants of the scalar-type four-quark and the KMT determinant interaction [52, 53], respectively, in which the determinant runs in flavor space. The KMT determinant interaction breaks the $U_A(1)$ symmetry explicitly.

The Polyakov-loop Φ and its conjugate Φ^* are determined

by

$$\Phi = \frac{1}{3} \text{tr}_c(L), \quad \Phi^* = \frac{1}{3} \text{tr}_c(\bar{L}), \quad (29)$$

where $L = \exp(iA_4/T)$ with $A_4/T = \text{diag}(\phi_r, \phi_g, \phi_b)$. Noting that $\phi_r + \phi_g + \phi_b = 0$, one can obtain

$$\begin{aligned} \Phi &= \frac{1}{3} (e^{i\phi_r} + e^{i\phi_g} + e^{i\phi_b}) \\ &= \frac{1}{3} (e^{i\phi_r} + e^{i\phi_g} + e^{-i(\phi_r + \phi_g)}), \\ \Phi^* &= \frac{1}{3} (e^{-i\phi_r} + e^{-i\phi_g} + e^{-i\phi_b}) \\ &= \frac{1}{3} (e^{-i\phi_r} + e^{-i\phi_g} + e^{i(\phi_r + \phi_g)}). \end{aligned} \quad (30)$$

We take the Polyakov potential of Ref. [20]:

$$\begin{aligned} \mathcal{U} = T^4 \left[-\frac{a(T)}{2} \Phi^* \Phi \right. \\ \left. + b(T) \ln(1 - 6\Phi\Phi^* + 4(\Phi^3 + \Phi^{*3}) - 3(\Phi\Phi^*)^2) \right], \end{aligned} \quad (31)$$

$$a(T) = a_0 + a_1 \left(\frac{T_0}{T}\right) + a_2 \left(\frac{T_0}{T}\right)^2, \quad b(T) = b_3 \left(\frac{T_0}{T}\right)^3. \quad (32)$$

Parameters of \mathcal{U} are determined to reproduce LQCD data at finite T in the pure gauge limit. The parameters except T_0 are summarized in Table I. The Polyakov potential yields the first-order deconfinement phase transition at $T = T_0$ in the pure gauge theory [54, 55]. The original value of T_0 is 270 MeV determined from the pure gauge LQCD data, but the PNJL model with this value of T_0 yields a larger value of the pseudocritical temperature T_c at zero chemical potential than $T_c \approx 160$ MeV predicted by full LQCD [56–58]. We then rescale T_0 to 195 MeV to reproduce $T_c = 160$ MeV [50].

a_0	a_1	a_2	b_3
3.51	-2.47	15.2	-1.75

TABLE I: Summary of the parameter set in the Polyakov-potential sector determined in Ref. [20]. All parameters are dimensionless.

Now we consider the flavor-dependent imaginary chemical potential $\mu_f = i\theta_f T$. The thermodynamic potential (per volume) based on the mean-field approximation is [42]

$$\begin{aligned} \Omega = & -2 \sum_{f=u,d,s} \sum_{c=r,g,b} \int \frac{d^3p}{(2\pi)^3} \left[E_f \right. \\ & + \frac{1}{\beta} \ln [1 + e^{i\phi_c} e^{i\theta_f} e^{-\beta E_f}] \\ & + \frac{1}{\beta} \ln [1 + e^{-i\phi_c} e^{-i\theta_f} e^{-\beta E_f}] \\ & \left. + U(\sigma_u, \sigma_d, \sigma_s) + \mathcal{U}(\Phi, \Phi^*, T) \right] \end{aligned} \quad (33)$$

with $\sigma_f \equiv \langle \bar{q}_f q_f \rangle$ and $E_f \equiv \sqrt{\mathbf{p}^3 + M_f^2}$ for $f = u, d, s$, where the three-dimensional cutoff is taken for the momentum integration in the vacuum term [42]. The dynamical quark masses M_f are defined by

$$M_f = m_f - 4G_S\sigma_f + 2G_D\sigma_{f'}\sigma_{f''} \quad (34)$$

for $f \neq f'$ and $f \neq f''$ and $f'' \neq f'''$. The mesonic potential $U(\sigma_u, \sigma_d, \sigma_s)$ are obtained by

$$U(\sigma_u, \sigma_d, \sigma_s) = \sum_{f=u,d,s} 2G_S\sigma_f^2 - 4G_D\sigma_u\sigma_d\sigma_s. \quad (35)$$

For the 2+1 flavor system with $m_u = m_d \equiv m_l$, the PNJL model has five parameters ($G_S, G_D, m_l, m_s, \Lambda$). A typical set is obtained in Ref. [59]. The parameter set is fitted to empirical values of η' -meson mass and π -meson mass and π -meson decay constant at vacuum. In the present paper, we set m_s to m_l in the parameter set of Ref. [59], since we consider the three degenerate flavor system with $m_0 \equiv m_l = m_s$. The parameter set is shown in Table II.

$m_0(\text{MeV})$	$\Lambda(\text{MeV})$	$G_S\Lambda^2$	$G_D\Lambda^5$
5.5	602.3	1.835	12.36

TABLE II: Summary of the parameter set in the NJL sector. All the parameters except m_0 are the same as in Ref. [59].

Taking the color summation in (33) leads to

$$\begin{aligned} \Omega = & -2 \sum_{f=u,d,s} \int \frac{d^3p}{(2\pi)^3} \left[N_c E_f \right. \\ & + \frac{1}{\beta} \ln[1 + C_{3,1}(\mathbf{p})e^{i\theta_f}] \\ & + C_{3,2}(\mathbf{p})e^{2i\theta_f} + C_{3,3}(\mathbf{p})e^{3i\theta_f}] \\ & + \frac{1}{\beta} \ln[1 + C_{3,1}^*(\mathbf{p})e^{-i\theta_f}e^{-\beta E_f} \\ & + C_{3,2}^*(\mathbf{p})e^{-2i\theta_f} + C_{3,3}^*(\mathbf{p})e^{-3i\theta_f}] \\ & \left. + U(\sigma_u, \sigma_d, \sigma_s) + \mathcal{U}(\Phi, \Phi^*, T), \right] \quad (36) \end{aligned}$$

where

$$\begin{aligned} C_{3,1}(\mathbf{p}) &= 3\Phi e^{-\beta E_f}, \\ C_{3,2}(\mathbf{p}) &= 3\Phi^* e^{-2\beta E_f}, \\ C_{3,3}(\mathbf{p}) &= e^{-3\beta E_f}. \end{aligned} \quad (37)$$

One can find that Ω has the RW periodicity,

$$\Omega(\theta_f) = \Omega(\theta_f + 2k\pi/3), \quad (38)$$

making the \mathbb{Z}_3 transformation,

$$\Phi \rightarrow e^{-i2\pi k/3}\Phi, \quad \Phi^* \rightarrow e^{i2\pi k/3}\Phi^*, \quad (39)$$

in Ω . In the case of $(\theta_u, \theta_d, \theta_s) = (\theta_1, \theta_1 + 2\pi/3, \theta_1 + 4\pi/3)$, Ω is invariant under the \mathbb{Z}_3 transformation, indicating that Ω

possesses the \mathbb{Z}_3 symmetry. When Φ vanishes, the color confinement ($C_{3,1} = C_{3,2} = 0$) occurs and thereby Ω has the flavor symmetry ($E_u = E_d = E_s$) since the factors $e^{\pm 3i\theta_f}$ have no flavor dependence in (36). The flavor symmetry is thus preserved by the color confinement ($\Phi = 0$) also for the case of $N_c = 3$.

B. Numerical results

First we consider the standard fermion boundary condition by setting $\theta_u = \theta_d = \theta_s = 0$. In this case, the σ_f are degenerate and hence $\sigma \equiv (\sigma_u + \sigma_d + \sigma_s)/3 = \sigma_f$. Figure 10 shows T dependence of σ and Φ . Both the chiral restoration and the deconfinement transition are crossover, although the former transition is a bit slower than the latter [50].

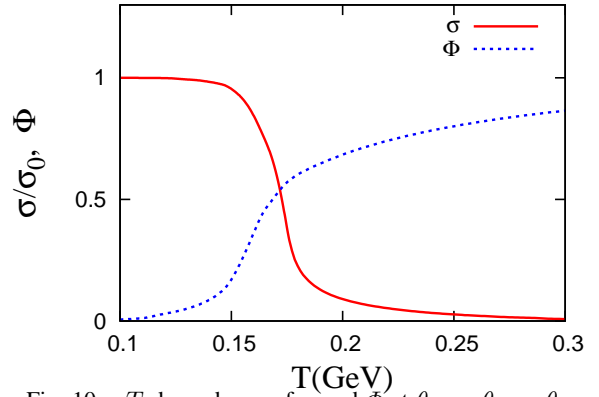


Fig. 10: T dependence of σ and Φ at $\theta_u = \theta_d = \theta_s = 0$. σ is normalized by σ_0 .

Next we consider the TBC model by taking two cases of $(\theta_u, \theta_d, \theta_s) = (0, 2\pi/3, 4\pi/3)$ and $(-\pi, -\pi/3, \pi/3)$ that correspond to the left and right panels in Fig. 11, respectively. The charge conjugation yields the relation

$$\Omega(\theta_u, \theta_d, \theta_s) = \Omega(-\theta_u, -\theta_d, -\theta_s) = \Omega(\theta_u, \theta_s, \theta_d) \quad (40)$$

for the two cases. Thus s-quark is symmetric with d-quark in these cases. Because of the \mathbb{Z}_3 symmetry, there are three \mathbb{Z}_3 vacua when $\Phi \neq 0$. We then take the solution in which a phase ϕ of Φ lies in a range of $-\pi/3 \leq \phi < \pi/3$. In the solution, Φ is found to be real.

Figure 12 shows T dependence of several physical quantities in the case of $(\theta_u, \theta_d, \theta_s) = (-\pi, -\pi/3, \pi/3)$. The order parameters Φ , σ and $a_0 \equiv \sigma_u - \sigma_d = \sigma_u - \sigma_s$ are plotted in panel (a). The first-order deconfinement transition takes place at $T = T_c \approx 195$ MeV. Below T_c , a_0 and Φ are zero. The flavor symmetry is thus preserved by the color confinement. Above T_c , a_0 and Φ become finite, indicating that the flavor and \mathbb{Z}_3 symmetries break simultaneously.

For the constituent quark masses M_f shown in panel (b), all the M_f are degenerate below T_c . Above T_c , M_u becomes heavier whereas two of the three, M_d and M_s , are degenerate and becomes lighter. The increase of M_u makes the chiral restoration slower. In panel (c), the absolute values of the

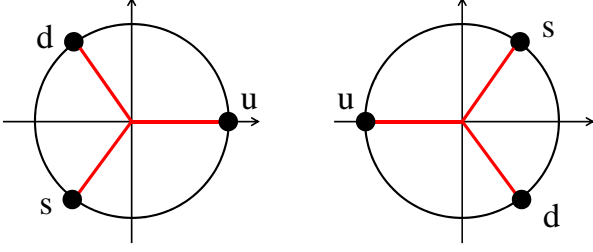


Fig. 11: Twisted factors $e^{i\theta_f}$ on a unit circle in the complex plane for the case of $\theta_1 = 0$ (left) and $\theta_1 = -\pi$ (right).

color-state factors $C_{3,1}$, $C_{3,2}$ and $C_{3,3}$ are plotted at $\mathbf{p} = 0$. Below T_c , $C_{3,3}$ is small but finite, whereas $C_{3,1} = C_{3,2} = 0$. Above T_c , the system is dominated by the one-quark state $C_{3,1}$.

Here the case of $(\theta_u, \theta_d, \theta_s) = (0, 2\pi/3, 4\pi/3)$ is considered briefly. As shown in Fig. 13, below $T_c \approx 195\text{MeV}$ physical quantities have the same properties as those in the previous case. The difference between the two cases appears above T_c . Particularly for M_f , it is found that $M_d = M_s > M_u$ in the present case, while $M_d = M_s < M_u$ in the previous case. Thus both d - and s -quarks becomes heavier as T increases from T_c . This property makes the chiral restoration even slower in the present case.

C. Two extensions of the TBC model

In this subsection, we extend the TBC model in two directions.

As the first extension, we use the entanglement PNJL (EPNJL) model [45, 50] instead of the PNJL model. A possible origin of the four-quark vertex G_S is a gluon exchange between quarks and its higher-order diagrams. If the gluon field A_ν has a vacuum expectation value $\langle A_0 \rangle$, A_ν is coupled to $\langle A_0 \rangle$ and hence to Φ through L [60]. This effect allows G_S to depend on Φ , namely $G_S = G_S(\Phi)$ [60]. It is expected that Φ dependence of $G_S(\Phi)$ will be determined in future by accurate methods such as the exact renormalization group method [60–62]. In this paper, however, we simply assume the following $G_S(\Phi)$ by respecting the chiral symmetry, the charge-conjugation symmetry [37] and the extended \mathbb{Z}_3 symmetry [2]:

$$G_S(\Phi) = G_S[1 - \alpha_1 \Phi \Phi^* - \alpha_2 (\Phi^3 + \Phi^{*3})]. \quad (41)$$

The PNJL model with the entanglement vertex (41) is called the EPNJL model [45, 50]. In principle, G_D can depend on Φ , too. However, Φ -dependence of G_D yields qualitatively the same effect on the phase diagram as that of G_S [50]. We then neglect Φ -dependence of G_D , following Ref. [50].

The parameters α_1 and α_2 in (41) are so determined as to reproduce two results of LQCD at finite T . The first is a result of 2+1 flavor LQCD at $\mu = 0$ [63] that the chiral transition is crossover at the physical point. The second is a result of

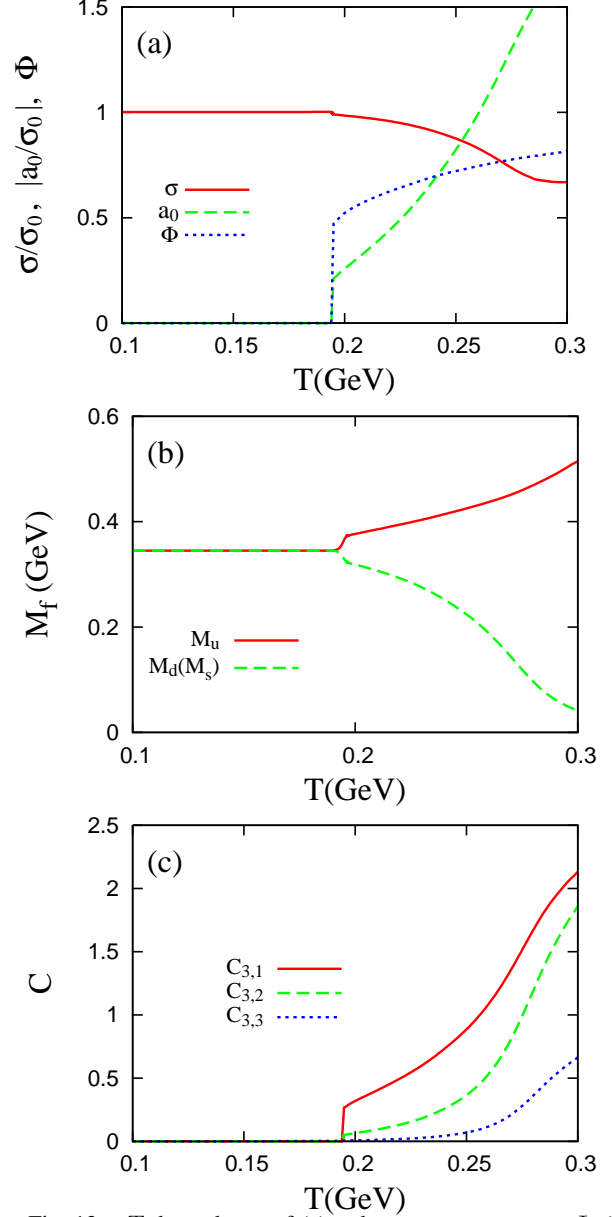


Fig. 12: T dependence of (a) order parameters σ , a_0 , Φ , (b) constituent quark masses M_f , (c) color-state factors $C_{3,1}$, $C_{3,2}$, $C_{3,3}$ at $\mathbf{p} = 0$ in the case of $(\theta_u, \theta_d, \theta_s) = (-\pi, -\pi/3, \pi/3)$. Here σ and a_0 are normalized by σ_0 . Note that $M_d = M_s$, $\sigma < 0$ and $a_0 \leq 0$.

degenerate three-flavor LQCD at $\theta = \pi$ [10] that the order of the RW endpoint is first-order for small and large quark masses but second-order for intermediate quark masses. The parameter set (α_1, α_2) satisfying these conditions is located in the triangle region [50]

$$\{-1.5\alpha_1 + 0.3 < \alpha_2 < -0.86\alpha_1 + 0.32, \alpha_2 > 0\}. \quad (42)$$

As a typical example, we take $\alpha_1 = 0.25$ and $\alpha_2 = 0.1$, following Ref. [50] and rescale T_0 to 150MeV [50].

Figure 14 shows T dependence of σ , a_0 and Φ calculated with the EPNJL model for (a) $(\theta_u, \theta_d, \theta_s) = (0, 0, 0)$ and (b)

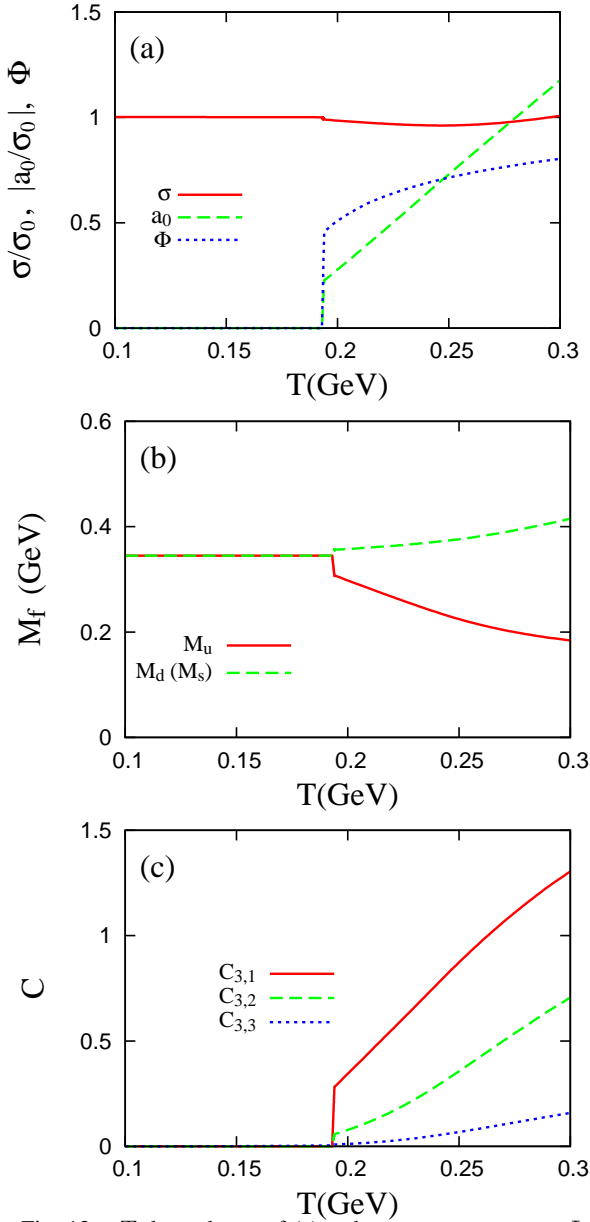


Fig. 13: T dependence of (a) order parameters σ , a_0 , Φ , (b) constituent quark masses M_f , (c) color-state factors $C_{3,1}$, $C_{3,2}$, $C_{3,3}$ at $\mathbf{p} = 0$ in the case of $(\theta_u, \theta_d, \theta_s) = (0, 2\pi/3, 4\pi/3)$. Here σ and a_0 are normalized by σ_0 . Note that $M_d = M_s$, $\sigma < 0$ and $a_0 \geq 0$.

$(\theta_u, \theta_d, \theta_s) = (0, 2\pi/3, 4\pi/3)$. In panel (a), the chiral restoration and the deconfinement transition are first-order, because of the small current quark mass (5.5MeV) and the strong correlation between σ_f and Φ [50]. In panel (b), the TBC model with the entanglement vertex yields similar T dependence to the EPNJL model with the standard quark boundary condition for the chiral restoration and the deconfinement transition, although the flavor symmetry is broken above T_c .

As the second extension of the TBC model with $N_f = N_c$, one can consider the TBC model with $N_f = lN_c$ for any positive integer l . It is obvious that the TBC model with $N_f = lN_c$ has the \mathbb{Z}_{N_c} symmetry, if the twisted angles θ_f are properly

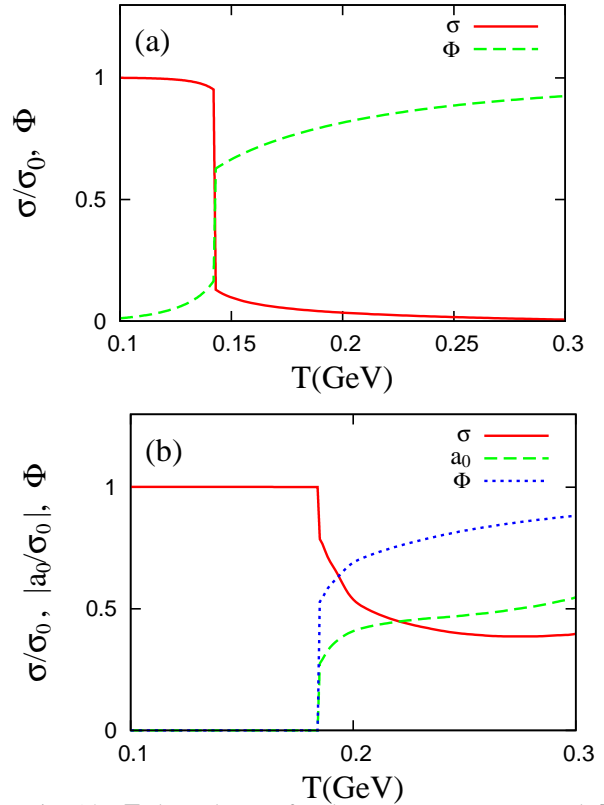


Fig. 14: T dependence of order parameters σ , a_0 and Φ calculated with the EPNJL model for (a) $(\theta_u, \theta_d, \theta_s) = (0, 0, 0)$ and (b) $(\theta_u, \theta_d, \theta_s) = (0, 2\pi/3, 4\pi/3)$. Here σ and a_0 are normalized by σ_0 . Note that $a_0 = 0$ in panel (a) and $a_0 \geq 0$ in panel (b), while $\sigma < 0$ in both panels.

ordered; for example,

$$\theta_f = \theta_1 + 2\pi(f-1)/N_f, \quad (43)$$

or

$$\theta_f = \theta_1 + 2\pi(f-1)/N_c, \quad (44)$$

for $f = 1, 2, \dots, N_f$.

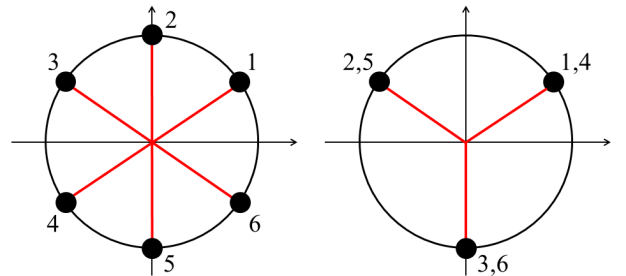


Fig. 15: Twisted factors $e^{i\theta_f}$ on a unit circle in the complex plane in the case of $N_c = 3$, $N_f = 6$ and $\theta_1 = \pi/6$. In the left and right panels, the $e^{i\theta_f}$ are obtained by (43) and (44), respectively.

Let us consider the case of $N_c = 3$, $N_f = 6$ and $\theta_1 = \pi/6$. In Fig. 15, the left and right panels show the twisted angles defined by (43) and (44), respectively. Here we take the right-panel case as an example. The thermodynamic potential Ω has the same form as (36), except the flavor summation is taken from $f = 1$ to 6. It is straightforward to show that Ω has the RW periodicity and the \mathbb{Z}_3 symmetry.

We take the same parameter set as in the case of $N_f = N_c = 3$, except G_s is taken as $G_S = G_{S,3} - G_{D,3}\sigma_f(0)/2 = 2.226 \text{ GeV}^2$, where $G_{S,3}$ and $G_{D,3}$ mean G_S and G_D in the case of $N_c = N_f = 3$, respectively, and $\sigma_f(0)$ stands for σ_f at $T = 0$ and $\theta_f = 0$ in the case of $N_c = N_f = 3$. We keep the Polyakov potential \mathcal{U} of (32), but neglect the KMT determinant interaction just for simplicity.

Figure 6 presents T dependence of σ_f and Φ for the right-panel case of Fig. 15. Below $T_c \approx 190 \text{ MeV}$, the flavor symmetry ($\sigma_1 = \sigma_2 = \dots = \sigma_6$) is preserved by the color confinement ($\Phi = 0$). Above T_c , the flavor and \mathbb{Z}_3 symmetries break simultaneously. The flavor symmetry breaking is partial because $f = 1$ is symmetric with $f = 4$, $f = 3$ with $f = 6$, and $f = 2$ with $f = 5$. As a consequence of this property, the σ_f split into three doublets.

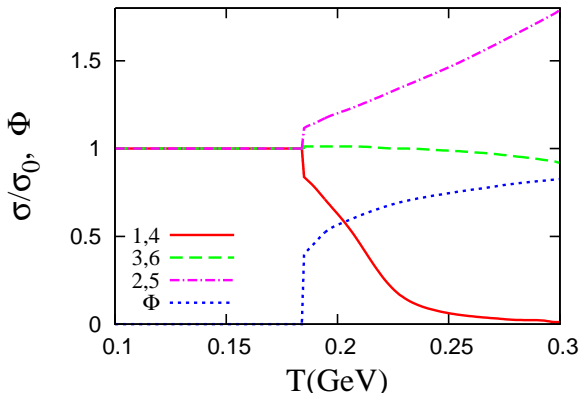


Fig. 16: T dependence of σ_f and Φ in the right-panel case of Fig. 15. The solid, dashed and dot-dashed lines represent $\sigma_1 = \sigma_4$, $\sigma_3 = \sigma_6$ and $\sigma_2 = \sigma_5$, respectively, whereas the dotted line corresponds to Φ .

IV. SUMMARY

We have proposed a QCD-like theory with the \mathbb{Z}_{N_c} symmetry. The QCD-like theory is constructed by imposing

the flavor-dependent twisted boundary condition (5) on the $SU(N_c)$ gauge theory with N_c degenerate flavor quarks. Dynamics of the QCD-like theory has been studied by imposing the TBC on the PNJL model. The TBC model has the \mathbb{Z}_{N_c} symmetry and hence the Polyakov loop becomes an exact order parameter of the deconfinement transition. The TBC model is a good model to investigate the mechanism of color confinement.

For both cases of $N_f = N_c = 2$ and 3, the Polyakov loop is zero up to some temperature T_c , but becomes finite above T_c . The \mathbb{Z}_{N_c} symmetry is thus preserved below T_c , but spontaneously broken above T_c . Below T_c , the color confinement preserves the flavor symmetry. Above T_c , meanwhile, the flavor symmetry is broken explicitly by the TBC. The flavor-symmetry breaking makes the chiral restoration slower, but the entanglement interaction between σ and Φ makes the restoration faster. The entanglement interaction thus suppresses the flavor symmetry breaking. In the standard-PNJL model with degenerate flavor quarks, Φ becomes finite but small at T lower than the pseudo-critical temperature, while the flavor symmetry is preserved. Dynamics of the TBC model is thus similar to that of the standard-PNJL model below T_c . The similarity is relatively worse above T_c , but it is improved by the entanglement interaction. One can then expect that QCD with the approximate \mathbb{Z}_3 symmetry is similar to the QCD-like theory with the \mathbb{Z}_3 symmetry and hence that the \mathbb{Z}_3 symmetry is a good approximate concept in QCD, even if the current quark mass is small.

The model prediction mentioned above can be tested with LQCD, since LQCD with the TBC has no sign problem. The QCD-like theory is useful to understand the mechanism of color confinement, since the \mathbb{Z}_{N_c} symmetry is exact. For example, it is quite interesting to see T dependence of the potential between q and \bar{q} in LQCD with the TBC.

Acknowledgments

The authors thank A. Nakamura, T. Saito, K. Nagata and K. Kashiwa for useful discussions. H.K. also thanks M. Imachi, H. Yoneyama, H. Aoki and M. Tachibana for useful discussions. T.S and Y.S. are supported by JSPS. The calculation was partially carried out on SX-8 at Research Center for Nuclear Physics, Osaka University.

[1] A. Roberge and N. Weiss, Nucl. Phys. **B275**, 734 (1986).
 [2] Y. Sakai, K. Kashiwa, H. Kouno, and M. Yahiro, Phys. Rev. D **77**, 051901(R) (2008); Phys. Rev. D **78**, 036001 (2008); Y. Sakai, K. Kashiwa, H. Kouno, M. Matsuzaki, and M. Yahiro, Phys. Rev. D **78**, 076007 (2008); K. Kashiwa, M. Matsuzaki, H. Kouno, Y. Sakai, and M. Yahiro, Phys. Rev. D **79**, 076008 (2009); K. Kashiwa, H. Kouno, and M. Yahiro, Phys. Rev. D **80**, 117901 (2009).

[3] P. de Forcrand and O. Philipsen, Nucl. Phys. **B642**, 290 (2002); P. de Forcrand and O. Philipsen, Nucl. Phys. **B673**, 170 (2003).
 [4] M. D'Elia and M. P. Lombardo, Phys. Rev. D **67**, 014505 (2003); Phys. Rev. D **70**, 074509 (2004); M. D'Elia, F. D. Renzo, and M. P. Lombardo, Phys. Rev. D **76**, 114509 (2007);
 [5] H. S. Chen and X. Q. Luo, Phys. Rev. D **72**, 034504 (2005); arXiv:hep-lat/0702025 (2007).

- [6] L. K. Wu, X. Q. Luo, and H. S. Chen, *Phys. Rev.* **D76**, 034505 (2007).
- [7] M. D'Elia and F. Sanfilippo, *Phys. Rev. D* **80**, 014502 (2009).
- [8] P. Cea, L. Cosmai, M. D'Elia, C. Manneschi and A. Papa, *Phys. Rev. D* **80**, 034501 (2009).
- [9] M. D'Elia and F. Sanfilippo, *Phys. Rev. D* **80**, 111501 (2009).
- [10] P. de Forcrand and O. Philipsen, arXiv:1004.3144 [hep-lat](2010).
- [11] K. Nagata, A. Nakamura, Y. Nakagawa, S. Motoki, T. Saito and M. Hamada, arXiv:0911.4164 [hep-lat](2009); K. Nagata, and A. Nakamura, arXiv:1104.2142 [hep-ph] (2011).
- [12] T. Takaishi, P. de Forcrand and A. Nakamura, arXiv:1002.0890 [hep-lat](2010).
- [13] G. Aarts, S. P. Kumar and J. Rafferty, *JHEP* **07**, 056 (2010); J. Rafferty, arXiv:1103.2315 [hep-th](2011).
- [14] P. N. Meisinger, and M. C. Ogilvie, *Phys. Lett. B* **379**, 163 (1996).
- [15] A. Dumitru, and R. D. Pisarski, *Phys. Rev. D* **66**, 096003 (2002); A. Dumitru, Y. Hatta, J. Lenaghan, K. Orginos, and R. D. Pisarski, *Phys. Rev. D* **70**, 034511 (2004); A. Dumitru, R. D. Pisarski, and D. Zschesche, *Phys. Rev. D* **72**, 065008 (2005).
- [16] K. Fukushima, *Phys. Lett. B* **591**, 277 (2004); *Phys. Rev. D* **77**, 114028 (2008).
- [17] C. Ratti, M. A. Thaler, and W. Weise, *Phys. Rev. D* **73**, 014019 (2006); C. Ratti, S. Rößner, M. A. Thaler, and W. Weise, *Eur. Phys. J. C* **49**, 213 (2007).
- [18] S. K. Ghosh, T. K. Mukherjee, M. G. Mustafa, and R. Ray, *Phys. Rev. D* **73**, 114007 (2006).
- [19] E. Megías, E. R. Arriola, and L. L. Salcedo, *Phys. Rev. D* **74**, 065005 (2006).
- [20] S. Rößner, C. Ratti, and W. Weise, *Phys. Rev. D* **75**, 034007 (2007).
- [21] Z. Zhang, and Y. -X. Liu, *Phys. Rev. C* **75**, 064910 (2007).
- [22] S. Mukherjee, M. G. Mustafa, and R. Ray, *Phys. Rev. D* **75**, 094015 (2007).
- [23] M. Ciminale, R. Gatto, N. D. Ippolito, G. Nardulli, and M. Ruggieri, *Phys. Rev. D* **77**, 054023 (2008); M. Ciminale, R. Gatto, G. Nardulli, and M. Ruggieri, *Phys. Lett. B* **657**, 64 (2007).
- [24] H. Hansen, W. M. Alberico, A. Beraudo, A. Molinari, M. Nardi, and C. Ratti, *Phys. Rev. D* **75**, 065004 (2007).
- [25] C. Sasaki, B. Friman, and K. Redlich, *Phys. Rev. D* **75**, 074013 (2007).
- [26] B. -J. Schaefer, J. M. Pawłowski, and J. Wambach, *Phys. Rev. D* **76**, 074023 (2007).
- [27] W. J. Fu, Z. Zhang, and Y. X. Liu, *Phys. Rev. D* **77**, 014006 (2008).
- [28] P. Costa, C. A. de Sousa, M. C. Ruivo, and H. Hansen, *Europhys. Lett.* **86**, 31001 (2009). P. Costa, M. C. Ruivo, C. A. de Sousa, H. Hansen, and W. M. Alberico, *Phys. Rev. D* **79**, 116003 (2009).
- [29] H. Abuki, M. Ciminale, R. Gatto, G. Nardulli, and M. Ruggieri, *Phys. Rev. D* **77**, 074018 (2008); H. Abuki, M. Ciminale, R. Gatto, N. D. Ippolito, G. Nardulli, and M. Ruggieri, *Phys. Rev. D* **78**, 014002 (2008).
- [30] H. Abuki, R. Anglani, R. Gatto, G. Nardulli, and M. Ruggieri, *Phys. Rev. D* **78**, 034034 (2008).
- [31] K. Kashiwa, H. Kouno, M. Matsuzaki, and M. Yahiro, *Phys. Lett. B* **662**, 26 (2008).
- [32] L. McLerran K. Redlich and C. Sasaki, *Nucl. Phys. A* **824**, 86 (2009).
- [33] Y. Sakai, K. Kashiwa, H. Kouno, M. Matsuzaki, and M. Yahiro, *Phys. Rev. D* **79**, 096001 (2009);
- [34] T. Brauner, K. Fukushima, and Y. Hidaka, *Phys. Rev. D* **80**, 074035 (2009).
- [35] T. Kähärä, and K. Tuominen, *Phys. Rev. D* **80**, 114022 (2009).
- [36] K. Kashiwa, M. Yahiro, H. Kouno, M. Matsuzaki, and Y. Sakai, *J. Phys. G: Nucl. Part. Phys.* **36**, 105001 (2009).
- [37] H. Kouno, Y. Sakai, K. Kashiwa, and M. Yahiro, *J. Phys. G: Nucl. Part. Phys.* **36**, 115010 (2009); H. Kouno, Y. Sakai, T. Sasaki, K. Kashiwa, and M. Yahiro, *Phys. Rev. D* **83**, 076009 (2011); H. Kouno, Y. Sakai, T. Sasaki, and M. Yahiro, *Phys. Rev. D* **85**, 016001 (2012).
- [38] T. Hell, S. Rößner, M. Cristoforetti, and W. Weise, *Phys. Rev. D* **81**, 074034 (2010); T. Hell, K. Kashiwa, and W. Weise, *Phys. Rev. D* **83**, 114008 (2011).
- [39] Y. Sakai, H. Kouno, and M. Yahiro, *J. Phys. G: Nucl. Part. Phys.* **37**, 105007 (2010).
- [40] A. Bhattacharyya, P. Deb, S. K Ghosh, and R. Ray, *Phys. Rev. D* **82**, 014021 (2010).
- [41] K. Fukushima, M. Ruggieri, and R. Gatto, *Phys. Rev. D* **81**, 114031 (2010).
- [42] T. Matsumoto, K. Kashiwa, H. Kouno, K. Oda, and M. Yahiro, *Phys. Lett. B* **694**, 367 (2011).
- [43] T. Sasaki, Y. Sakai, H. Kouno, and M. Yahiro, *Phys. Rev. D* **82**, 116004 (2010); Y. Sakai, T. Sasaki, H. Kouno, and M. Yahiro, *Phys. Rev. D* **82**, 096007 (2010).
- [44] C. A. Contrera, M. Orsaria, and N. N. Scoccola, *Phys. Rev. D* **82**, 054026 (2010). V. Pagura, D. Gomez Dumm, and N. N. Scoccola, arXiv:1105.1739 [hep-ph](2011).
- [45] Y. Sakai, T. Sasaki, H. Kouno, and M. Yahiro, *Phys. Rev. D* **82**, 076003 (2010).
- [46] R. Gatto, and M. Ruggieri, *Phys. Rev. D* **83**, 034016 (2011).
- [47] K. Kashiwa, *Phys. Rev. D* **83**, 117901 (2011).
- [48] K. Kashiwa, T. Hell, and W. Weise, arXiv:1106.5025 [hep-ph](2011).
- [49] K. Morita, V. Skokov, B. Friman, and K. Redlich, arXiv:1107.2273 [hep-ph](2011); arXiv:1108.0735 [hep-ph](2011).
- [50] T. Sasaki, Y. Sakai, H. Kouno, and M. Yahiro, *Phys. Rev. D* **84**, 091901 (2011);
- [51] Y. Sakai, T. Sasaki, H. Kouno, and M. Yahiro, *J. Phys. G* **39**, 035004 (2012).
- [52] M. Kobayashi, and T. Maskawa, *Prog. Theor. Phys.* **44**, 1422 (1970); M. Kobayashi, H. Kondo, and T. Maskawa, *Prog. Theor. Phys.* **45**, 1955 (1971).
- [53] G. 't Hooft, *Phys. Rev. Lett.* **37**, 8 (1976); *Phys. Rev. D* **14**, 3432 (1976); **18**, 2199(E) (1978).
- [54] G. Boyd, J. Engels, F. Karsch, E. Laermann, C. Legeland, M. Lütgemeier, and B. Petersson, *Nucl. Phys.* **B469**, 419 (1996).
- [55] O. Kaczmarek, F. Karsch, P. Petreczky, and F. Zantow, *Phys. Lett. B* **543**, 41 (2002).
- [56] S. Borsányi, Z. Fodor, C. Hoelbling, S. D. Katz, S. Krieg, C. Ratti, and K. K. Szabo, arXiv:1005.3508 [hep-lat] (2010).
- [57] W. Söldner, arXiv:1012.4484 [hep-lat] (2010).
- [58] K. Kanaya, arXiv:hep-ph/1012.4235 [hep-ph] (2010); arXiv:hep-ph/1012.4247 [hep-lat] (2010).
- [59] P. Rehberg, S.P. Klevansky and J. Hüfner, *Phys. Rev. C* **53**, 410 (1996).
- [60] K.-I. Kondo, *Phys. Rev. D* **82**, 065024 (2010).
- [61] J. Braun, L. M. Haas, F. Marhauser, and J. M. Pawłowski, *Phys. Rev. Lett.* **106**, 022002 (2011); J. Braun, and A. Janot, arXiv:1102.4841 [hep-ph] (2011).
- [62] C. Wetterich, *Phys. Lett. B* **301**, 90 (1991).
- [63] Y. Aoki, G. Endrödi, Z. Fodor, S. D. Katz and K. K. Szabó, *Nature* **443**, 675 (2006).